OPEN ACCESS



Features of Magnetic Field Switchbacks in Relation to the Local-field Geometry of Largeamplitude Alfvénic Oscillations: Wind and PSP Observations

Sofiane Bourouaine ¹ , Jean C. Perez ² , Nour E. Raouafi ¹ , Benjamin D. G. Chandran ³ , Stuart D. Bale ⁴ , and Marco Velli ⁵

Johns Hopkins Applied Physics Laboratory, 11100 Johns Hopkins Road, Laurel, MD, 20723, USA; sofiane.bourouaine@jhuapl.edu
Department of Aerospace, Physics and Space Sciences, Florida Institute of Technology, 150 W University Blvd, Melbourne, Fl, 32901, USA
Department of Physics and Astronomy, University of New Hampshire, Durham, NH 03824, USA
Space Sciences Laboratory, University of California, Berkeley, CA 94720, USA
Earth, Planetary, and Space Sciences, University of California, Los Angeles, Los Angeles, CA 90095, USA
Received 2022 January 25; revised 2022 April 5; accepted 2022 April 17; published 2022 June 17

Abstract

In this Letter, we report observations of magnetic switchback (SB) features near 1 au using data from the Wind spacecraft. These features appear to be strikingly similar to the ones observed by the Parker Solar Probe mission closer to the Sun: namely, one-sided spikes (or enhancements) in the solar-wind bulk speed V that correlate/anticorrelate with the spikes seen in the radial-field component B_R . In the solar-wind streams that we analyzed, these specific SB features near 1 au are associated with large-amplitude Alfvénic oscillations that propagate outward from the Sun along a local background (prevalent) magnetic field B_0 that is nearly radial. We also show that, when B_0 is nearly perpendicular to the radial direction, the large-amplitude Alfvénic oscillations display variations in V that are two sided (i.e., V alternately increases and decreases depending on the vector $\Delta B = B - B$). As a consequence, SBs may not always appear as one-sided spikes in V, especially at larger heliocentric distances where the local background field statistically departs from the radial direction. We suggest that SBs can be well described by large-amplitude Alfvénic fluctuations if the field rotation is computed with respect to a well-determined local background field that, in some cases, may deviate from the large-scale Parker field.

Unified Astronomy Thesaurus concepts: Heliosphere (711); Solar wind (1534)

1. Introduction

Near the Sun, at heliocentric distances below 20.17 au, the Parker Solar Probe (PSP; Fox et al. 2016) observes many intervals of slow wind where the bulk flow suddenly increases associated with temporary radial magnetic field reversals. These observed features were interpreted as magnetic switchbacks (SBs) (e.g., Bale et al. 2019; Kasper et al. 2019; Dudok de Wit et al. 2020). Also, these observed SBs are characterized by a high degree of Alfvénicity. The word "Alfvénicity" is commonly related to the characteristics of Alfvén waves (with finite or small amplitude), which are an exact solution to the magnetohydrodynamics (MHD) equations (Walén 1944; Goldstein et al. 1974; Barnes & Hollweg 1974). These Alfvén waves are characterized by the following properties: (1) They satisfy Walén relations, $\Delta V = \pm \Delta B / \sqrt{\mu_0 \rho}$, where ΔV and ΔB are velocity and magnetic field perturbations around the background, respectively, and μ_0 is the vacuum's magnetic permeability; (2) they have constant mass density, ρ , constant pressure, p, and constant magnetic field strength, |B|; and (3) they propagate with a group velocity, called the Alfvén velocity, $V_A = \pm B_0 / \sqrt{\mu_0 \rho}$, either parallel (for $\Delta V = -\Delta B / \mu_0 \rho$) or antiparallel (for $\Delta V = +\Delta B / \mu_0 \rho$) to the local background magnetic field B₀. Several in situ measurements have revealed the existence of Alfvén waves in the solar wind that propagate mainly outward from the Sun (see, e.g., Bavassano et al. 1998), which means the perturbed fields ΔV

Original content from this work may be used under the terms of the Creative Commons Attribution 4.0 licence. Any further distribution of this work must maintain attribution to the author(s) and the title of the work, journal citation and DOI.

and ΔB either anticorrelate (when B > 0) or positively correlate (when $B_{0R} < 0$). Here B_{0R} is the component of B_0 along the radial direction pointing outward from the Sun.

SBs have been previously observed over a wide range of heliocentric distances (see, e.g., Borovsky 2016), near 0.3 au (Horbury et al. 2018), near 1 au (Kahler et al. 1996; Gosling et al. 2009), and beyond 1 au (Balogh et al. 1999; Yamauchi et al. 2004; Neugebauer & Goldstein 2013). In PSP observations, the electron Strahl pitch angle distributions were found to follow the magnetic field through SBs (Whittlesey et al. 2020). Also, within SBs, Alfvénic fluctuations at inertial-range scales appear to have correlations corresponding to fluctuations propagating toward the Sun (Bourouaine et al. 2020; McManus et al. 2020).

Several scenarios have been proposed to explain the origin of SBs. Some studies suggest that SBs are caused by magnetic reconnection as a result of interchange between open and closed magnetic field structures at the base of the solar corona, which are then convected outward with the solar wind (e.g., Fisk & Kasper 2020; Zank et al. 2020; Drake et al. 2021; Liang et al. 2021). Other scenarios propose that SBs are created locally in the solar wind as a result, for example, of the radial evolution of Alfvénic turbulence in the expanding solar wind (Landi et al. 2006; Squire et al. 2020; Mallet et al. 2021; Shoda et al. 2021) or due to shear-driven dynamics (see e.g., Landi et al. 2006; Ruffolo et al. 2020; Schwadron & McComas 2021).

Unlike some previous works in which SBs are attributed to field deflections with respect to the large-scale Parker field (see, e.g., Balogh et al. 1999; Matteini et al. 2014; Borovsky 2016), in this Letter we analyze the field rotation with respect to a local background field, which may deviate from the large-scale

Parker spiral due to the presence of large-scale fluctuations (e.g., waves having periods of a few days Coleman 1968).

In this Letter, we use Wind data to show that some of the SB features observed recently by PSP near the Sun, such as the one-sided spikes (or enhancements) in the bulk flow that correlate/anticorrelate with the spikes seen in the radial component of the magnetic field, are also observed near 1 au (where the large-scale Parker field is not nearly radial). Here, we demonstrate that such SB features seem to show up naturally when large-amplitude Alfvénic oscillations propagate antisunward along a nearly radial (or antiradial) local prevalent field. Those SB features are also compared with the ones observed by PSP during its first perihelion. In the following section, we present the analysis method and our findings. Then, in Section 3, we summarize and discuss the obtained results.

2. Data Analysis and Results

We use plasma and field measurements from Wind to investigate the presence of SB features near 1 au. We use the combined data of the magnetic field vector and the plasma parameters provided with a time resolution of about 24.7 s (Lepping et al. 1995). Here the vector fields are given in the Geocentric Solar Ecliptic system (GSE), i.e., the x-axis pointing from Earth toward the Sun, the y-axis is chosen to be in the ecliptic plane pointing toward dusk (opposing planetary motion), and the z-axis is parallel to the ecliptic north. For the sake of comparison with SBs observed by PSP, we will also use plasma and magnetic field data from PSP during its first encounter (Bale et al. 2016; Case et al. 2020). The PSP data shown here are provided in the radialtangential-normal (RTN) coordinate system. Here, we lower the resolution of PSP data to the plasma resolution of Wind, namely, 24.7 s for a better comparison.

Figure 1 displays the results from an 8 hr long time interval on 2002 January 12 of Wind measurements. Panels (a) and (b) show the histograms of the azimuthal angle f and the polar angle θ , respectively. The azimuthal angle f is defined as the angle between the radial direction outward from the Sun (-x direction) and the projected component of B onto the x-y plane, and the polar angle θ is the angle between the polar axis, z, and the instantaneous vector field B. From the histogram plots, the most prevalent values of both angles correspond to f; 5° and θ ; 86°. Here, the local mean field B₀ (averaged over the 8 hr long time interval) field is nearly radial (nearly parallel to the bulk velocity) and lies nearly on the ecliptic plane.

Panel (c) of Figure 1 displays the normalized x-component of the field $B_x/|B| = -B_R/|B|$ (where B_R is the radial component) versus time. The normalized x-component $B_x = -B_R$ oscillates in a one-sided fashion, showing the kind of spikes that at some points can even exceed zero value and flip the sign. In the same figure, we plot the flow speed V (purple line) that also oscillates in a one-sided fashion following the spikes in $-B_R/|B|$. Panel (d) of Figure 1 shows that the spikes in B_x are mostly associated with the deviations of the angles f and θ from their prevalent values.

As shown in panel (e) of Figure 1 these field oscillations occur at nearly constant B² and constant Alfvén speed, $V_A = B / \sqrt{\mu_0 \rho}$, where ρ is the mass density of protons. These are highly Alfvénic oscillations with a normalized cross-helicity of $\sigma_c = -0.9$, where $\sigma_c = 2 \langle (\Delta V \cdot \Delta \hat{B}) / (\Delta V^2 + \Delta \hat{B}^2) \rangle$, and

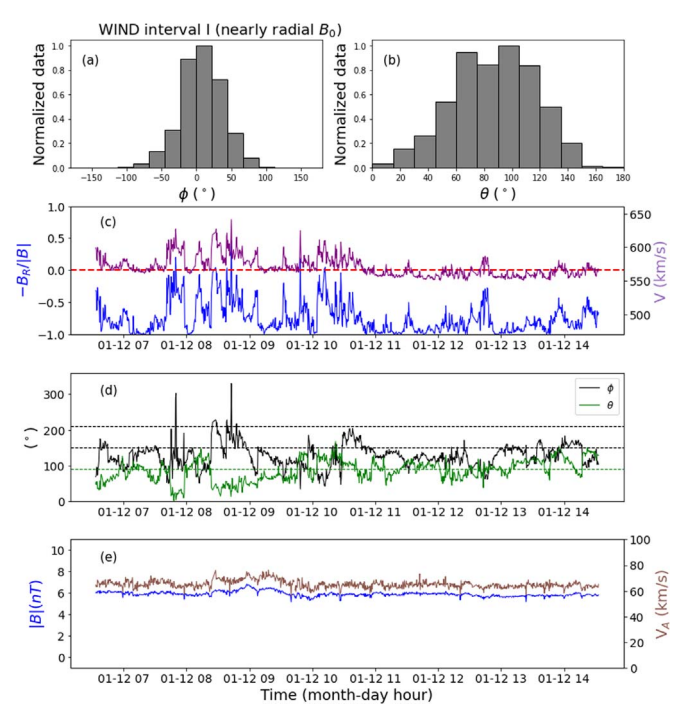


Figure 1. 8 hr long time interval I of Wind observations. Panels from top to bottom correspond to (a) and (b) histograms of the f and θ angle, respectively, (c) the normalized radial component of the magnetic field $-B_R/|B|$ (blue line) and the bulk flow V (purple line), (d) the azimuthal angle f (black) and the polar angle θ (green), respectively, and (e) the magnitude of the magnetic field vector |B| (blue) and the Alfvén speed V_A (brown).

 ΔV = V - V_0 ($\Delta \hat{\pmb{B}} = (\pmb{B} - \pmb{B}_0) \big/ \sqrt{\mu_0 \rho_0}$) is the fluctuating velocity field (magnetic field, converted to velocity unit). Here, V_0 and ρ_0 are the mean quantities (averaged over the 8 hr long time interval) of the velocity and mass density, respectively. The Alfvénic structures measured in this interval propagate outward from the Sun (as $\sigma_c < 0$ and $-B_{0x} = B_{0R} > 0$).

The features shown in Figure 1 appear to be similar to the ones observed by PSP near the Sun at $\mathbb{Z}0.17$ au (see, e.g., Bale et al. 2019; Kasper et al. 2019). For the sake of comparison, in Figure 2, we plot the same parameters as those shown in Figure 1 but from an 8 hr long time interval of PSP during its first encounter on 2018 November 2 and 3. Analysis of this interval shows that the local background field is nearly antiradial corresponding to a prevalent azimuthal angle $f = 175^{\circ}$ (and $\theta = 88^{\circ}$). Here the f angle is defined with respect to the radial axis of an RTN coordinate system, with $B_R \equiv -B_x$. The oscillations of the radial component B_R correlate with the one-sided enhancement in the bulk flow. These oscillations are also highly Alfvénic (with $\sigma_c = 0.9$) and propagate outward from the Sun (as $\sigma_c > 0$ and $B_{0R} < 0$.)

In order to check how the geometry of the local background magnetic field may affect the overall features that are often associated with SBs near the Sun, we select another 8 hr long time interval observed by Wind (shown in Figure 3) in which the oscillations are also highly Alfvénic (with $\sigma_c = -0.9$) and the local mean field is nearly perpendicular to the radial direction (and the solar wind bulk velocity). From the top panels of Figure 3, we see that the most frequent value of $f(\theta)$ is 2100° (293°) corresponding to a local background field B_0 that is nearly perpendicular to the radial direction. In this case, the Alfvénic oscillations propagate antiparallel to B_0 .

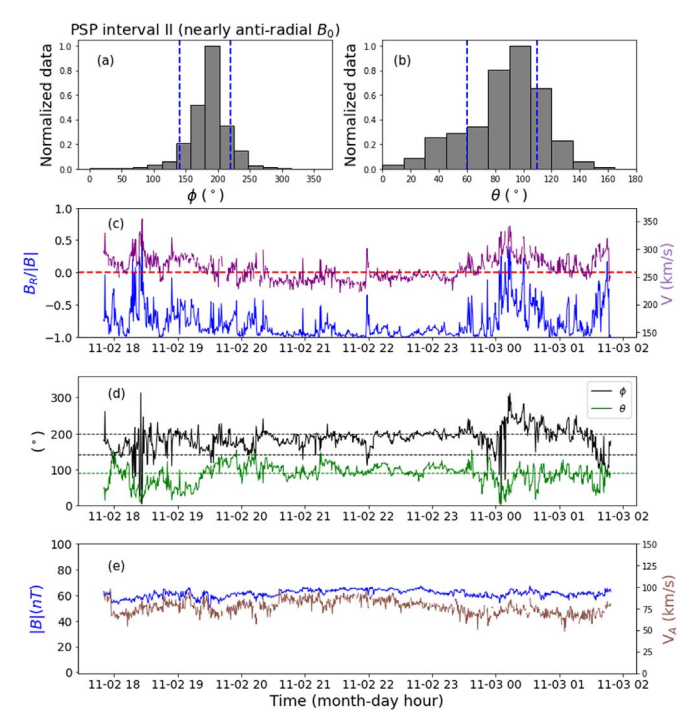


Figure 2. 8 hr long time interval II of PSP measurements. Panels from top to bottom correspond to (a) and (b) histograms of the f and θ angle, respectively, (c) the normalized radial component of the magnetic field $B_R/|B|$ (blue line) and the bulk flow V (purple line), (d) the azimuthal angle f (black) and the polar angle θ (green), respectively, and (e) the magnitude of the magnetic field vector |B| (blue) and the Alfvén speed V_A (brown).

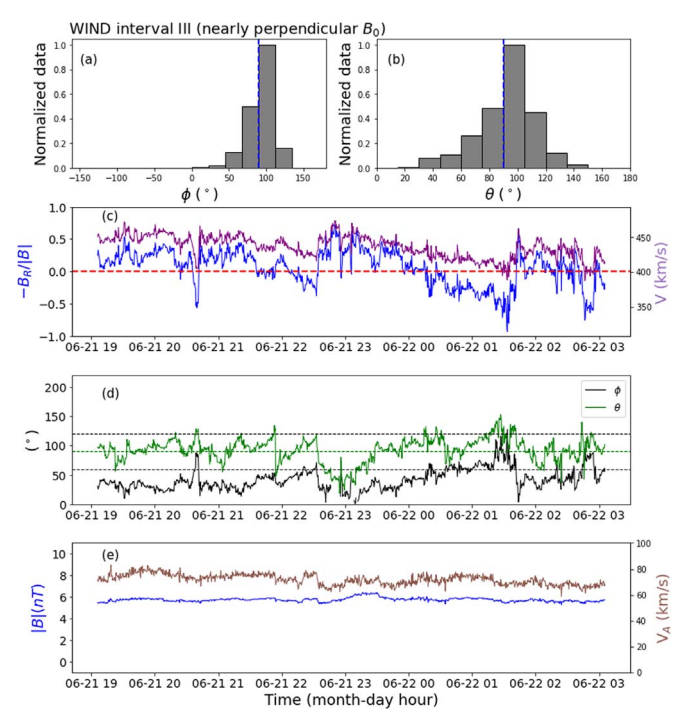
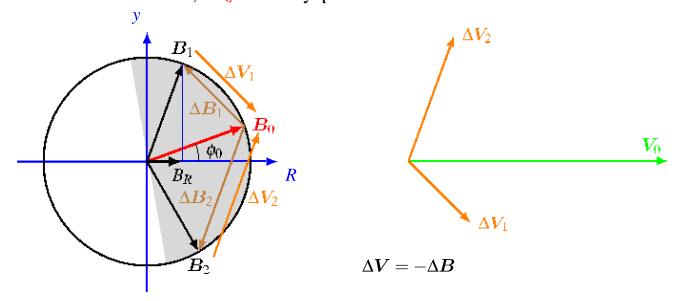


Figure 3. Interval III of Wind measurements. Panels from top to bottom correspond to (a) and (b) histograms of the f and θ angle, respectively, (c) the normalized radial component of the magnetic field $-B_R/|B|$ (blue line) and the bulk flow V (purple line), (d) the azimuthal angle f (black) and the polar angle θ (green), respectively, and (e) the magnitude of the magnetic field vector |B| (blue) and the Alfvén speed V_A (brown).

For this geometrical configuration of the local field B_0 , the bulk flow and the radial component of the field do not show one-sided spikes as seen in Figures 1 and 2.

a) B_0 is nearly parallel to the radial direction



b) B_0 is nearly perpendicular to the radial direction

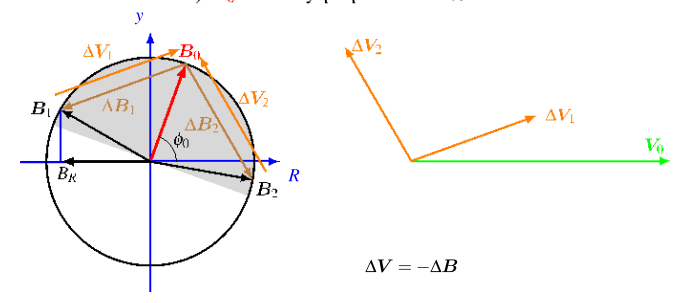
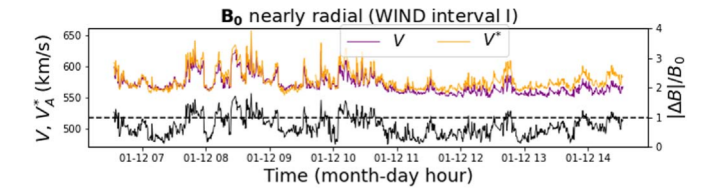
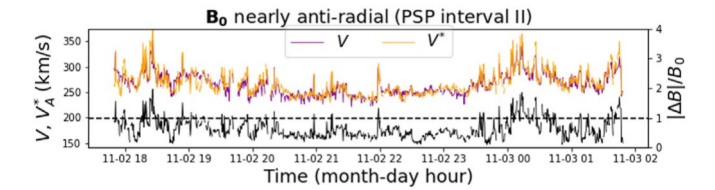


Figure 4. Sketch describes how the radial-field component $B_{\nu}/|B|$ and the fluctuating bulk velocity $\Delta V_1 = -\Delta B_1$ and $\Delta V_2 = -\Delta B_2$ (orange vectors) add to the local mean bulk velocity V_0 (Green vector) during the oscillation of the instantaneous magnetic field vector B_1 and B_2 (black vectors) around the local background magnetic field vector B_0 for the case (a) where B_0 is nearly radial and for case (b) where B_0 is nearly perpendicular to the radial direction (of the bulk flow direction). Here ΔB_1 and ΔB_2 are normalized to velocity units.

In the following we propose a picture, illustrated in Figure 4, to explain how the local background field direction and the corresponding antisunward Alfvénic oscillations (in the case when B_0 is nearly radial or antiradial) may provide the above patterns of the bulk flow and the radial component of the field. For the sake of simplicity, we assume that the local background field B_0 and the oscillating field vector B both lie nearly in the ecliptic plane. The demonstration below can still hold even when the oscillating field B is out of the ecliptic (i.e., with polar angle $\theta \neq 90^{\circ}$).

Figure 4(a) shows the case when the instantaneous magnetic field B (shown in black) oscillates in the shaded area around a nearly radial prevalent (background) magnetic field B₀ (shown in red), nearly parallel to the mean bulk flow velocity, V_0 , shown in green). If we assume that these oscillations are purely Alfvénic and propagate outward from the Sun, then the fluctuating magnetic field vector $\Delta \hat{\mathbf{B}} = (\mathbf{B} - \mathbf{B}_0) / \sqrt{\mu_0 \rho}$ and the fluctuating bulk velocity vector $\Delta \mathbf{V} = \mathbf{V} - \mathbf{V}_0$ have opposite signs, i.e., $\Delta V = -\Delta B$ (in units where $\sqrt{\mu_0 \rho_z} = 1$). Here V is the instantaneous measured bulk flow vector. In this case, because the magnetic field is nearly radial, the instantaneous field B oscillates around B o within the shaded area, producing the vector changes ΔB_1 (counterclockwise) and ΔB_2 (clockwise). In such rotations of B the radial component B_R/|B| (here |B| is constant) varies between positive and negative values for some large rotations near or larger than 90°, leading to the kind of one-sided oscillations in B_{p} that we see in the second panels of Figures 1 and 2. Interestingly, in this B₀ configuration, it seems that the fluctuating velocity vectors $\Delta V_1 = -\Delta B_1$ and $\Delta V_2 = -\Delta B_2$ (orange vectors) both contribute to the enhancement of the bulk flow V_0 , leading to one-sided increases of the bulk flow that





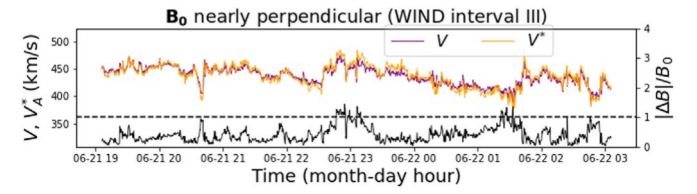


Figure 5. Panels from top to bottom correspond to the measured bulk flow V (purple line) and the bulk flow V^* reconstructed from changes in the magnetic field ΔB for intervals I, II, and III. The horizontal dashed line represents the mean bulk flow V_0 considered for the reconstruction of V^* .

correlate with the spikes of $-B_R$. Note that this explanation holds even when B_0 is nearly antiradial and $\sigma_c > 0$ for antisunward propagating Alfvénic oscillations, except that the one-sided increases of the bulk flow correlate with the spikes of B_n .

 B_R . However, when the local background field B_0 is nearly perpendicular to the radial direction (or to the bulk velocity), then the oscillating instantaneous field B around B_0 can cover a wide range in which the radial component B_R oscillates between positive and negative values in more or less equivalent ways. In such a case, the B_R component will not show a onesided pattern as shown in the second panel of Figure 3. Moreover, the counterclockwise (clockwise) rotation of the field B with respect to B_0 produces a change in the velocity ΔV_1 (ΔV_2) that leads to either an increase (decrease) in the bulk velocity when $\sigma_c \! < \! 0$ (or either decrease (increase) in the bulk velocity when $\sigma_c \! > \! 0$) for such a B_0 geometry.

To further verify the picture given above, we estimate the fluctuating bulk velocity, ΔV^* , from the empirical fluctuating magnetic field $\triangle B$ as $\triangle V^* = \alpha \triangle B$ (in units where $\sqrt{\mu_0 \rho} = 1$), where $\alpha = -1$ ($\alpha = 1$) when B₀ is near radial (antiradial). This approximate estimation is based on the assumption that the oscillations are entirely Alfvénic and with antisunward propagation at least for the case when B₀ is nearly radial or antiradial. Therefore, we estimate the modeled bulk flow, V*, as $V^* = |V_0 + \Delta V^*|$ for the three intervals we used above. Here V_0 is the mean bulk flow velocity. Figure 5 displays the velocity V*, obtained from the model (orange line), and the bulk flow V (purple line) obtained from direct measurements for the three intervals I (Wind), II (PSP) and III (Wind) used in Figures 1, 2, and 3, respectively. Figure 5 shows that the modeled velocity, V*, and the empirical bulk flow V nearly overlap. It is clear that the enhanced bulk flow in most parts of the signal in the two top panels can be well explained by the propagation of Alfvén waves along a nearly radial local background field B₀ for the Wind and the PSP measurements. In addition, in the bottom

3. Summary and Discussion

Matteini et al. (2014) studied the dependence of solar wind speed on the magnetic field orientation in Alfvénic solar wind streams at high latitudes. The authors proposed that the enhancement in the bulk flow depends on the position of the instantaneous field B with respect to a local mean field that is not assumed to be radial (but nearly follows the Parker field direction at 1 au). In our analysis, we instead focused on the geometry of the local background field, B₀, of Alfvénic oscillations and showed how that geometry affects the profile of the solar wind bulk flow when the field rotates strongly with respect to B₀.

From our analysis, we conjecture that SBs (or at least a subset of SBs) can be sudden large rotations of the field (with $|\Delta B|/B_0 \mathbb{Z}$ 1) associated with large-amplitude Alfvénic oscillations that propagate outward from the Sun along a well-determined local background field, but this local field may in some cases deviate from the Parker spiral due to the presence of larger-scale solar wind oscillations, e.g., oscillations with periods of days (Coleman 1968; Bruno & Carbone 2005). Also, the one-sided spikes in the bulk flow speed that often appear to correlate/anticorrelate with the radial magnetic field component cannot be used as the main criterion for the determination of SB field reversals.

SBs (or at least a subset of them) are strongly connected to large-amplitude Alfvénic oscillations, which therefore makes understanding the evolution of the large-amplitude Alfvénic fluctuations in the solar wind a necessary part of understanding the dynamics and evolution of SBs. For example, recent studies proposed that these types of oscillations can be generated by the solar wind expansion (e.g., Squire et al. 2020; Mallet et al. 2021).

The authors would like to thank Dr. C. H. K. Chen for his valuable discussions. SB was supported by NASA grants 80NSSC21K0012 and Parker Solar Probe as part of NASA's Living with a Star (LWS) program (contract NNN06AA01C). JCP was partially supported by NASA grant 80NSSC21K0012 and NSF grant AGS-1752827. BDGC was supported in part by NASA grants NNN06AA01C and 80NSSC19K0829.

ORCID iDs

Sofiane Bourouaine https://orcid.org/0000-0002-2358-6628 Jean C. Perez https://orcid.org/0000-0002-8841-6443 Nour E. Raouafi https://orcid.org/0000-0003-2409-3742 Benjamin D. G. Chandran https://orcid.org/0000-0003-4177-3328

Stuart D. Bale to https://orcid.org/0000-0002-1989-3596 Marco Velli to https://orcid.org/0000-0002-2381-3106

References

```
Bale, S. D., Badman, S. T., Bonnell, J. W., et al. 2019, Natur, 576, 237
Bale, S. D., Goetz, K., Harvey, P. R., et al. 2016, SSRv, 204, 49
Balogh, A., Forsyth, R. J., Lucek, E. A., Horbury, T. S., & Smith, E. J. 1999,
   GeoRL, 26, 631
Barnes, A., & Hollweg, J. V. 1974, JGR, 79, 2302
Bavassano, B., Pietropaolo, E., & Bruno, R. 1998, JGR, 103, 6521
Borovsky, J. E. 2016, JGRA, 121, 5055
Bourouaine, S., Perez, J. C., Klein, K. G., et al. 2020, ApJL, 904, L30
Bruno, R., & Carbone, V. 2005, LRSP, 2, 4
Case, A. W., Kasper, J. C., Stevens, M. L., et al. 2020, ApJS, 246, 43
Coleman, P. J. J. 1968, ApJ, 153, 371
Drake, J. F., Agapitov, O., Swisdak, M., et al. 2021, A&A, 650, A2
Dudok de Wit, T., Krasnoselskikh, V. V., Bale, S. D., et al. 2020, ApJS,
  246, 39
Fisk, L. A., & Kasper, J. C. 2020, ApJL, 894, L4
Fox, N. J., Velli, M. C., Bale, S. D., et al. 2016, SSRv, 204, 7
```

```
Goldstein, M. L., Klimas, A. J., & Barish, F. D. 1974, in Solar Wind Three, On
   the theory of large amplitude Alfvén waves, ed. C. T. Russell, 385, https://
  www.osti.gov/servlets/purl/4137645
Gosling, J. T., McComas, D. J., Roberts, D. A., & Skoug, R. M. 2009, ApJL,
  695, L213
Horbury, T. S., Matteini, L., & Stansby, D. 2018, MNRAS, 478, 1980
Kahler, S. W., Crooker, N. U., & Gosling, J. T. 1996, JGR, 101, 24373
Kasper, J. C., Bale, S. D., Belcher, J. W., et al. 2019, Natur, 576, 228
Landi, S., Hellinger, P., & Velli, M. 2006, GeoRL, 33, L14101
Lepping, R. P., Acuna, M. H., Burlaga, L. F., et al. 1995, SSRv,
   71, 207
Liang, H., Zank, G. P., Nakanotani, M., & Zhao, L. L. 2021, ApJ,
  917, 110
Mallet, A., Squire, J., Chandran, B. D. G., Bowen, T., & Bale, S. D. 2021, ApJ,
  918, 62
Matteini, L., Horbury, T. S., Neugebauer, M., & Goldstein, B. E. 2014,
   GeoRL, 41, 25
McManus, M. D., Bowen, T. A., Mallet, A., et al. 2020, ApJS, 246, 67
Neugebauer, M., & Goldstein, B. E. 2013, in AIP Conf. Ser. 1539, Solar Wind
   13, ed. G. P. Zank et al. (New York: AIP), 46
Ruffolo, D., Matthaeus, W. H., Chhiber, R., et al. 2020, ApJ, 902, 94
Schwadron, N. A., & McComas, D. J. 2021, ApJ, 909, 95
Shoda, M., Chandran, B. D. G., & Cranmer, S. R. 2021, ApJ, 915, 52
Squire, J., Chandran, B. D. G., & Meyrand, R. 2020, ApJL, 891, L2
Walén, C. 1944, ArMAF, 30A, 1
Whittlesey, P. L., Larson, D. E., Kasper, J. C., et al. 2020, ApJS, 246, 74
Yamauchi, Y., Suess, S. T., Steinberg, J. T., & Sakurai, T. 2004, JGRA, 109,
Zank, G. P., Nakanotani, M., Zhao, L. L., Adhikari, L., & Kasper, J. 2020, ApJ,
```